processes

MDPI

Article

Design and Verification of Two-Stage Brake Pressure Servo Valve for Aircraft Brake System

Lilei Zhang [1], Zhipeng Huang [2], Chengwei Fu [2], Yuepeng Xu [2], Yunhe Wang [2] and Xiangdong Kong [2,*]

[1] College of Horticulture and Landscape Architecture, Henan University of Science and Technology, Xinxiang 453000, China; zhll1232021@163.com
[2] School of Mechanical Engineering, Yanshan University, Qinhuangdao 066004, China; zhipengh@stumail.ysu.edu.cn (Z.H.); fcw@stumail.ysu.edu.cn (C.F.); stuyuepeng@stumail.ysu.edu.cn (Y.X.); wangyunhe@stumail.ysu.edu.cn (Y.W.)
* Correspondence: xdkong@ysu.edu.cn

Abstract: Wheel braking devices is some of the most widely used landing deceleration devices in modern aircraft. Jet pipe pressure servo valves are widely used in large aircraft wheel brake control systems because of their high anti-pollution ability, high sensitivity and fast dynamic response. However, most brake systems suffer vibration phenomena during the braking process. The pressure servo valve is an important part of the hydraulic brake system, and also an important factor affecting the vibration of the system. In order to solve the vibration problem in the brake system this paper present a two-stage brake pressure servo valve design. We place feedback channels at both ends of the main spool to stabilize the output pressure. In addition, modeling, simulation and experimental verifications are carried out. Firstly, the principle and structure of the pressure servo valve are described. An accurate mathematical model of the two-stage brake pressure servo valve and the testing system is established. Then a simulation analysis is carried out. Finally, a two-stage brake pressure servo valve testing experimental platform system is built for experimental verification. The experimental results show that the mathematical model of the two-stage brake pressure servo valve and the test system established in this paper have high accuracy, and the designed servo valve structure can restrain vibrations. The above research results provide a useful theoretical reference for performance optimization, stability analysis and valve body structure improvement of brake pressure servo valves.

Keywords: aircraft brake system; two-stage pressure servo valve; accurate modeling; vibration suppression

Citation: Zhang, L.; Huang, Z.; Fu, C.; Xu, Y.; Wang, Y.; Kong, X. Design and Verification of Two-Stage Brake Pressure Servo Valve for Aircraft Brake System. *Processes* **2021**, *9*, 979. https://doi.org/10.3390/pr9060979

Academic Editor: Cesar De Prada

Received: 6 April 2021
Accepted: 29 May 2021
Published: 1 June 2021

1. Introduction

With the progress of science and technology, large aircraft technology has become an important field leading the development of modern industry, which involves a wide range of technical fields and rich content, attracting a large number of scholars for research. In the control system of large aircraft, the wheel brake control system is one of the subsystems with independent functions. With the rapid development of aviation technology, modern aircraft is constantly developing towards the direction of higher load and higher performance. The test of the effectiveness and safety of the brake system is especially important [1]. In order to obtain stable brake output pressure, a large number of experts and scholars have conducted in-depth research. Zhang, from the perspective of suppressing the vibration of hydraulic system pipeline, divided the vibration of aircraft brake control system into four categories: gear-walk, whirl, chatter and squeal. He elaborated on their respective characteristics, frequency range and destructive consequences [2]. Based on the rolling mill, Yongshun analyzed the inducement of vibration [3]. Shang established a model to analyze the aircraft brake valve noise vibration and successfully predicted the system vibration under the condition of fixed friction coefficient. At the same time, he proposed corresponding

vibration suppression measures for cyclotron vibration and howling vibration [4]. The above research is mainly aimed at some key components of the brake control system.

Servo valves are mainly divided into jet pipe servo valves and nozzle baffle servo valves [5,6]. Through understanding the key technology of jet pipe servo valves, it is found that there are many kinds of jet pipe servo valve. These mainly include rotary jet pipe servo valves, jet pipe valves, integrated jet pipe valves, slide valve end inclined jet pipe valves and middle jet pipe valves [7–18]. To verify the adaptability of jet pipe valves in aircraft braking systems, Yang [19] and Zhao [20] compared the performance indexes of nozzle flapper valves and jet pipe valves, and proposed that the key technical indexes of jet pipe valves meet the performance requirements of nozzle flapper valves. Zhang [21] provided an experimental method for the stability assessment of jet pipe valves with experimental projects as the background. In order to study the influence of main structural parameters on the performance of jet pipe valves Yi [22] built a jet pipe valve simulation platform with the AMESim software, and analyzed the influence of the main structural parameters on the characteristics of jet pipe valves, which provided a theoretical basis for the design of the valves. To study the dynamic characteristics of servo valves, Berri [23] built a valve-controlled cylinder system, but the servo valve was simplified as an inertial link, which cannot truly reflect the dynamic characteristics of the servo valve. The servo valve model built by Hao [24] is divided into two levels to restore the structure of the servo valve. However, the use of linearization parameters masks the dynamic changes of output pressure. Lin [25] built a servo valve model, where the parameters of the model are fitted according to the experiment, which can really express the dynamic characteristics of the servo valve. Most scholars have made substantial progress in the research on jet pipe servo valves, but research on the design of servo valves and how to solve its vibration issues is less common. The model we built mainly takes into account various factors that cause vibration. Firstly, it is necessary to accurately model each part of the servo valve. The effect of all feedback channels also needs to be considered. Finally, the overall model of a valve-controlled cylinder system is built. This is unprecedented.

During the braking process of the aircraft, passengers often feel "washboard" and jitter instability effects. Especially in military aircraft, pilots feel that the brake jitter and vibration are more obvious. When this vibration is serious, it can cause brake failure and landing gear fatigue damage and other consequences. In order to analyze and verify the vibration, it is necessary to establish a high-precision modeling analysis of the servo valve, which is helpful to the development of jet pipe servo valves in the field of high-precision control.

To solve the above problems, this paper designs a two-stage brake pressure servo valve (TSBPSV) for aircraft brake systems and carries out accurate modeling and experimental verification. The innovative achievements of this work are as follows:

(1) A novel structure of two-stage pressure servo valve is proposed in this paper. By setting feedback channels, the degenerative feedback effect on the displacement of the main valve core is realized, which can stabilize the output pressure and effectively restrain the vibration during the process of braking.
(2) According to the principle of the TSBPSV designed in this paper, a matching mathematical model is established, the effect of vibration suppression of the valve is simulated and analyzed, and an experimental platform is built to verify the simulation results.

This paper is organized as follows: In Section 2 the principle of the TSBPSV and its test system are introduced. In Section 3, an accurate dynamic model of the TSBPSV and control cylinder system are established, including torque motor, jet pipe amplifier, power stage spool, load actuator and oil return channel. In Section 4, the model is simulated and analyzed, and the step response and slope response are tested. In Section 5, the TSBPSV and its test system are verified by experiments. In Section 5.1, an experimental platform is built. In Section 5.2, the system pressure output under two kinds of response is tested to

verify the accuracy of the dynamic model of the TSBPSV cylinder system. Section 6 is the summary of this paper.

2. Introduction of TSBPSV and Test System Principle

2.1. Structure Principle of TSBPSV

In view of the vibration phenomenon existing in aircraft brake servo system, a TSBPSV structure is proposed. The feedback channels at both ends of the main valve core in the structure can effectively restrain the vibration phenomenon, as shown in Figure 1.

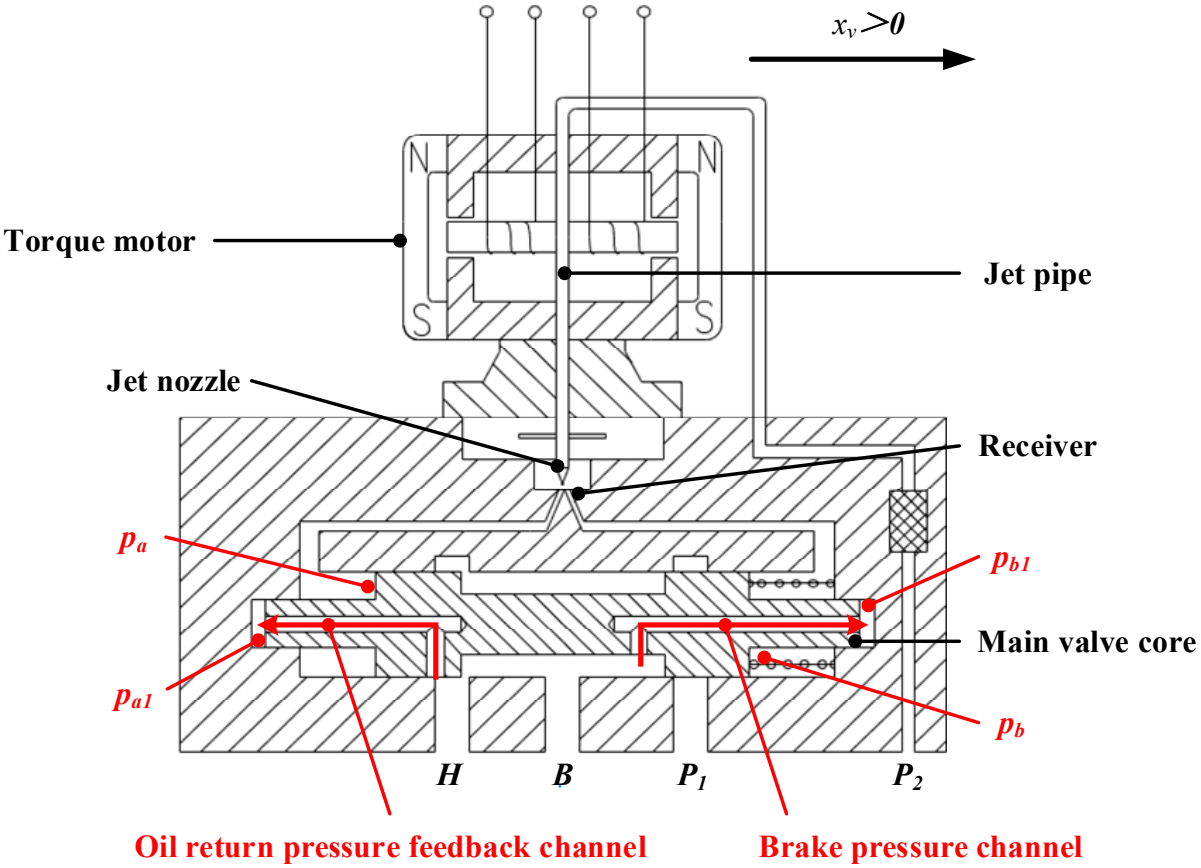

Figure 1. TSBPSV structure.

As shown in Figure 1, the working principle of TSBPSV is as follows: When the torque motor does not receive the current signal, the jet pipe does not deflect. Therefore, the flow of the jet nozzle enters the left and right holes of the receiver, and the control pressure $p_a = p_b$. At the same time, the brake pressure channel and the oil return pressure feedback channel are connected with the oil return port H. That is, the feedback pressure on both sides of the main valve spool $p_{a1} = p_{b1} = p_h$. The right spring makes the main spool at the leftmost. At this time, the brake port B is connected with the oil return port H.

When the torque motor receives the current signal, the armature will drive the jet pipe to deflect clockwise. The flow of the jet nozzle enters the left receiving hole more than the right. At this time, $p_a > p_b$, so the main valve spool moves to the right. Port B is connected port P_1 and disconnected from port H. Thus, pressure oil enters the brake actuator through port B. At this time, the feedback pressure $p_{b1} > p_{a1}$. This produces a force to the left of the spool, which forms a stable inverse feedback effect. The valve port between port B and port P_1 decreases and the brake pressure decreases.

Due to the pressure change during the brake pressure control process, PB1 is too large. At this time, B is connected with H but disconnected from P_1. As a result, the brake pressure decreases and the return pressure increases. p_{a1} is increased and p_{b1} decreased.

A stable inverse feedback is formed, and further inverse movement of the main spool is hindered. In the working process, the feedback channel forms a inverse feedback effect on the spool movement. In this way, stable brake pressure output is finally formed.

2.2. Introduction to the Principle of TSBPSV Test System

The hydraulic principle of the TSBPSV testing system is shown in Figure 2. The hydraulic cylinder 12.1 on the left is connected with the pressure servo valve 10 through the hydraulic hose as the actuator in the system. The pressure sensor 11.1 is used to collect the output pressure of the pressure servo valve and transfer it to the controller. The hydraulic cylinder 12.2 on the right, force sensor 13, servo valve 14, controller 8.2 and amplifier 9.2 jointly constitute the electro-hydraulic load simulator. Due to the presence of the force sensor, the precise control of the load can be realized. The two-position three-way directional control valves 15.1 and 15.2 are used to control the on-off of the brake pressure servo valve and the oil circuit of the load simulation unit, respectively. The accumulator 7 and the normally open globe valve 1.2 form a pressure regulating module to stabilize the pressure pulsation from the hydraulic oil source. Oil return relief valve 16, pressure sensor 11.2 and controller 8.3 form the oil return back pressure unit, which is used to set the back pressure of the system and transmit the real-time data of oil return back pressure to controller. The flood valve 4, normally open stop valve 1.3 and pressure gauge 18 are used to set the outlet pressure of the hydraulic pump. High pressure fine filter 5 is installed at the pump port to clean the oil. Servo motor 3 drives axial piston quantitative pump 2 to provide oil source. Air cooler 17 is used to cool oil.

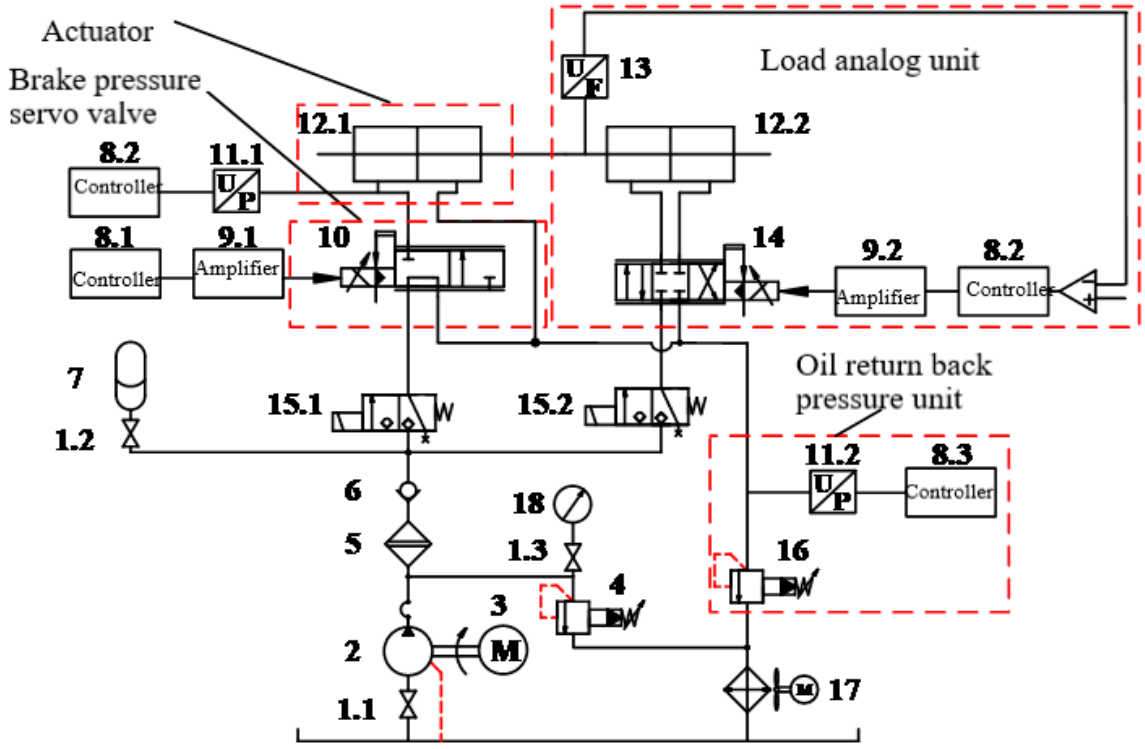

Figure 2. Hydraulic principle of TSBPSV test system. 1—Globe valve; 2—Axial piston quantitative pump; 3—Servo motor; 4—Flood valve; 5—Filter; 6—Check valve; 7—Accumulator; 8—Controller; 9—Amplifier; 10, 14—Servo valve; 11—Pressure sensor; 12—Hydraulic c cylinder; 13—Force sensor; 15—Two position three—way reversing valve; 16—Return oil relief valve; 17—Air cooler; 18—Pressure gauge.

The modeling of the TSBPSV testing system consists of three key parts, namely, the two-stage pressure servo valve dynamic model, the load actuator dynamic model and

the oil return channel dynamic model composed of the oil return pipe and the oil return relief valve.

3. Modeling of TSPBSV and Test System

In order to analyze the vibration suppression effect of the TSPBSV, the mathematical and dynamic simulation models of TSPBSV and the test system were established. In the modeling process of TSBPSV test system, the dynamic model of load actuator and oil return channel are considered.

3.1. Mathematical Modeling of Torque Motor

Torque motor is the electro-mechanical converter commonly used in electro-hydraulic servo valve. The TSBPSV proposed in this paper adopts a permanent magnet torque motor TSBPSV. The effect of the feedback stage spool on the spring tube and feedback rod assembly is considered when establishing the dynamic model. The relationship between output torque of torque motor, control current and armature deflection angle is established as follows [26]:

$$T_d = K_t \cdot \Delta i + K_m \cdot \theta \tag{1}$$

The balance equation of armature feedback component is as follows [26]:

$$T_d = J_a \frac{\mathrm{d}^2\theta}{\mathrm{d}t^2} + B_a \frac{\mathrm{d}\theta}{\mathrm{d}t} + K_a\theta \tag{2}$$

When the jet nozzle deflects in a small range, k_q and k_c can be obtained by calculating the coincidence area of the receiving holes. The comprehensive characteristic equation is as follows [26]:

$$Q_f = k_q r\theta - k_c p_L \tag{3}$$

The load pressure equation of the jet amplifier is as follows:

$$p_l = \frac{\beta}{V_{cv}}\left(Q_f - A_1 x_v\right) \tag{4}$$

where, T_d is the electromagnetic moment (Nm); θ is the deflection angle of jet pipe (rad); K_m is the magnetic torque spring stiffness (N/m); Δi is the control current (A); K_t is the electromagnetic moment coefficient (Nm/A); J_a is the moment of inertia of armature jet pipe assembly (kg/m^2); Ba is the damping coefficient of armature jet pipe assembly (Nm/rad/s); K_a is spring tube stiffness (Nm/rad); Q_f is the load flow rate of jet nozzle (m^3/s); k_q is the linear flow coefficient of jet nozzle (m^2/s); k_c is the linear flow rate/pressure gradient of jet nozzle (m^3/s). r is the length of jet nozzle (m); P_l is the load pressure of the jet amplifier (Pa). β is the bulk elastic modulus of the oil (Pa); V_{cv} is the outlet cavity of jet nozzle (m^3); A_1 is the area acting on the load pressure of the jet amplifier (m^2); x_v is the power level spool displacement (m).

3.2. Power Level Valve Core Mathematical Model

The new structure of the valve is that there are feedback channels at both ends of the main spool, which are connected with the oil return port and the pressure oil, respectively. When modeling, it is necessary to consider the feedback pressure of the spool in different positions, and the dynamic equation of the power stage spool is established as follows:

$$p_L A_1 + p_h A_2 - p_b A_2 = M_v \frac{d^2 x_v}{dt^2} + B_v \frac{dx_v}{dt} + K(x_v + x_{v0}) + K_f x_v \tag{5}$$

$$Q = C_d W x_v \sqrt{\frac{2}{\rho} p_{vL}} \tag{6}$$

where, A_2 is the pressure feedback area of the power level spool (m^2); M_v is the power level spool mass (kg); B_V is the damping coefficient of the power level spool (Nm/rad/s); K is the spring stiffness of the power level spool (N/m); X_{v0} is the initial compression of the power level spool spring (m); K_f is the steady-state hydraulic dynamic stiffness of the power level spool (N/m); C_d is the flow coefficient of the power level spool; W is the displacement of the spool at the power level (m); Q is the load flow rate of the power level spool (m^3/s); P_{vL} is the power level spool load differential pressure (Pa).

3.3. Mathematical Modeling of Load Actuator

In this paper, the load characteristics of the TSBPSV are described according to the power-stage load flow equation, the flow continuity equation of the brake actuator and the dynamic equation of the brake actuator.

As shown in Figure 1, when $x_v > 0$, the oil flows into the rod-less cavity of the brake actuator through the right throttle window of the middle shoulder of the power stage spool to form a load flow, and the flow rate is positive. When $x_v < 0$, the oil enters the oil return chamber through the left throttle window of the middle shoulder of the power stage spool, and the flow rate is inverse. Therefore, the load flow at the power level of the brake pressure servo valve is as follows:

$$Q_L = C_d W x_v \sqrt{\frac{2}{\rho}\left(\frac{1+sign(x_v)}{2}p_s + \frac{-1+sign(x_v)}{2}p_h - sign(x_v)p_b\right)} \tag{7}$$

where, Q_l is the load flow rate (m^3/s).

The load flow has three main functions after entering the brake actuator, including pushing the piston rod to motion, compensating for leakage, causing the pressure rise. Therefore, it can be obtained from the flow continuity equation as follows:

$$Q_L = A_g\frac{dy}{dt} + \frac{V_{gb}}{\beta}\frac{\mathrm{d}p_b}{\mathrm{d}t} + C_b p_b \tag{8}$$

where, A_g is the effective area of the piston of the brake actuator (m^2); y is the displacement of the piston rod of the brake actuator (m); V_{gb} is the brake cavity (m^3) composed of the rodless cavity of the brake actuator and the hydraulic pipe. C_b is leakage coefficient of brake actuator ($m^3/s{\cdot}Pa$).

The first item on the right of Equation (8) is the volume change of the rod-less cavity caused by the displacement of the piston rod of the brake actuator. The velocity of the piston rod can be solved according to the dynamic equation of the brake actuator as follows:

$$A_g p_b = M_g\frac{\mathrm{d}^2y}{\mathrm{d}t^2} + B_g\frac{\mathrm{d}y}{\mathrm{d}t} + K_g y \tag{9}$$

where, M_g is the mass of the actuator piston (kg); B_g is the viscosity damping coefficient of the actuator piston (Nm/rad/s); K_g is the actuator spring stiffness (N/m).

3.4. Mathematical Modeling of Oil Return Channel

The oil return channel of the brake pressure servo valve control cylinder system is not directly connected to the oil tank. Instead, it is a series oil return back pressure valve to simulate 0.6 MPa fixed back pressure of self-pressurized fuel tank in aircraft hydraulic system. Oil return back pressure valve can be realized by throttle valve, relief valve, etc. In this paper, the relief valve with better pressure stabilization performance was selected. The selected DBD direct-acting relief valve is shown in Figure 3.

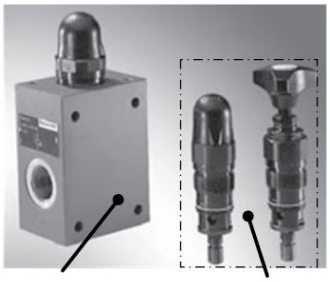

Figure 3. The DBD type relief valve.

DBD type direct-acting relief valve insert body structure is shown in Figure 4. It is mainly composed of pressure regulating element 1, valve sleeve 2, spring 3 and conical spool 4, the pressure of the system can be set with the help of the pressure regulating element. Its working principle is as follows: spring 3 presses conical spool 4 on the seat, channel P is connected to the H port of the brake pressure servo valve through the pipeline., The oil return pressure of the system acts on the cavity 6 at the bottom of the valve core through the internal damping hole to form a static pressure opposite to the spring force. If the value exceeds the set value of the spring, the spool 4 overcomes the spring force and opens. Among them, the stroke of the spool is limited by the limit slot 5.

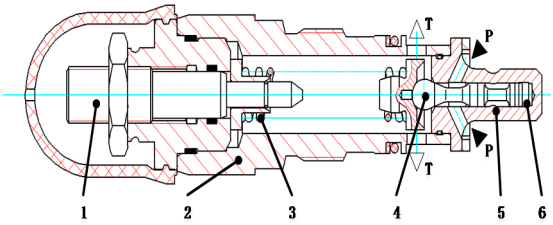

Figure 4. The insert part structure of DBD type relief valve.

To express the dynamic behavior of the relief valve more intuitively, the Figure 4 is simplified to the form shown in Figure 5.

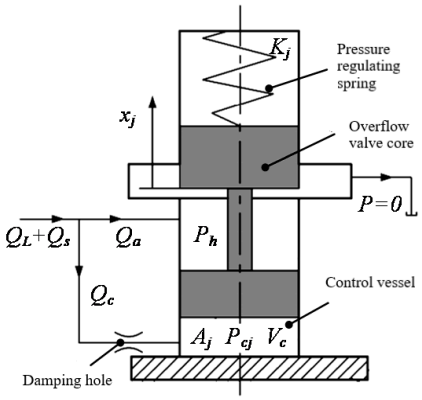

Figure 5. The principle of DBD type relief valve.

The dynamic model of oil return relief valve can be described by the following equations. The flow continuity equation of relief valve spool is shown as follows:

$$\dot{p}_h = \frac{\beta}{V_h}\left(Q_a - A(x_j)C_{dj}\sqrt{\frac{2}{\rho}p_h}\right) \tag{10}$$

where, $\dot{p}_h$ refers to control pressure change of relief valve (Pa/s);$A(x_j)$ is the flow area of the relief valve port (m^2)); C_{dj} is the flow coefficient of the relief valve; x_j is the displacement of the spool of the relief valve (m); Q_a is the overflow valve flow (m^3/s).

For a DBD type direct acting relief valve, its spool structure is a cone valve. When the spool moves, the relative position between the spool and the valve seat is as shown in Figure 6.

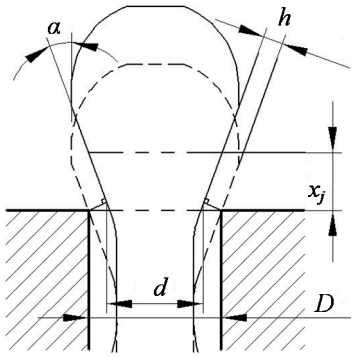

Figure 6. The relief valve spool relative position.

The over-flow area of the relief valve core can be calculated by Equation (11):

$$\begin{aligned} A(x_j) &= \pi dh = (D - 2h\cos\alpha)\pi h = (D - 2x_j\sin\alpha\cos\alpha)\pi x_j\sin\alpha \\ &= \left(1 - \tfrac{x_j}{D}\sin 2\alpha\right)\pi D x_j\sin\alpha \end{aligned} \tag{11}$$

where, D is the diameter of the relief valve port (m); α is the spool cone Angle (°).

When the spool displacement is small, there is $A(x_j) = \pi D x_j \sin\alpha$.

The flow continuity equation of the control cavity is shown as follows:

$$\dot{p}_{cj} = \frac{\beta}{V_{cj}}(Q_c - A_j\dot{x}_j) \tag{12}$$

where, $\dot{p}_{cj}$ refers to pressure change of relief valve (Pa/s); V_{cj} is the volume of the overflow valve control chamber (m^3); Q_c is to control the flow rate of the cavity for the relief valve (m^3/s); A_j is the area (m^2) of the relief valve control pressure. β is the damping coefficient (Nm/rad/s).

The spool of the relief valve is in dynamic balance under the action of oil return pressure, spring force, damping force of the spool and inertia force of the spool. The dynamic equation of relief valve spool is shown as follows:

$$p_{cj}A_j = M_j\ddot{x}_j + B_j\dot{x}_j + K_jx_j + K_jx_{j0} + k_sx_jp_h \tag{13}$$

where, k_s is the steady-state fluid dynamic coefficient of the spool of the relief valve (N/mPa); M_j is the mass of the moving parts of the relief valve (kg); B_j is the relief valve damping coefficient (Nm/rad/s); K_j is the relief valve pressure regulating spring stiffness (N/m); x_{j0} is the initial compression of the relief valve pressure regulating spring (m).

We now establish the flow equation of damping hole. Under the action of pressure difference, the flow through the damping hole is shown as follows:

$$Q_c = R_c(p_h - p_{cj}) \tag{14}$$

$$R_c = \frac{\pi\delta^4}{128\mu l} \tag{15}$$

where, R_C is the impedance of the relief valve damping hole ($m^3/s{\cdot}Pa$); δ is the flood valve damping aperture (m); μ is the dynamic viscosity of oil (m^2/s); l is the length of the relief valve damping hole (m).

The total flow equation of the relief valve is shown as follows:

$$Q_L + Q_s = Q_a + Q_c \tag{16}$$

where, Q_s is the flow rate of jet nozzle (m^3/s).

4. Simulation Analysis of Brake Pressure Servo Valve

According to the key components of the TSBPSV and the mathematical model of the test system, using the simulation parameters in Table 1, the dynamics simulation model of the TSBPSV and the test system is built on the MATLAB/Simulink software platform, as shown in Figure 7.

Table 1. Simulation parameter value.

K_t	J_a	B_a	K_a	K_m	K_q	K_c
0.9 Nm/A	5.5×10^{-7} kg·m^2	0.005 Nm/rad/s	21.5 Nm/rad	13.1 Nm/rad	0.02 N/m	6×10^{-13} N/m
A_1	A_2	K_f	K_d	M_g	B_g	K_g
1.93×10^{-5} m^2	1.25×10^{-5} m^2	0.0124 N/m	8.5×10^{-4} N/m	13.1 N/s	50 N/s^2	1×10^6 N/m
A_g	C_b	E	X_{v0}	V_{gb}	V_{cv}	K
6.15×10^{-4} m^2	2.38×10^{-13}	1.7×10^9	0	2×10^{-4} m^3	1.9^{-4} m^3	0.06N/m

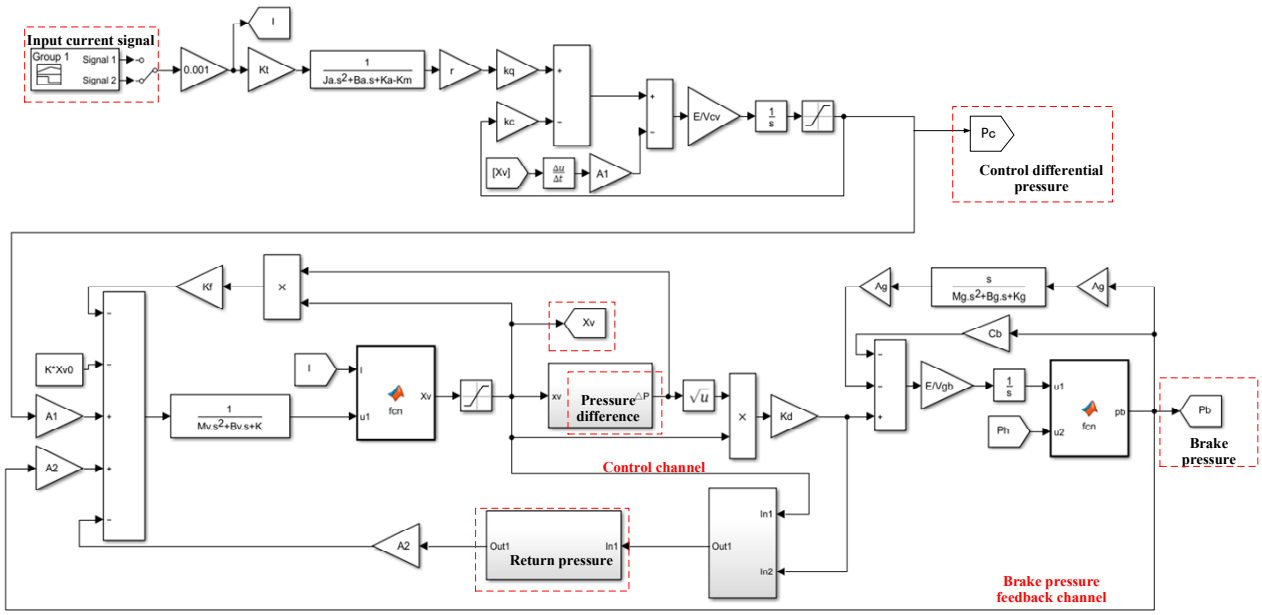

Figure 7. The MATLAB/Simulink model of new brake pressure servo valve-actuator system.

The current signal is input to the pilot stage of servo valve. In addition, the control pressure is input to A_2 through the feedback channel, and ΔP is obtained through Formula (13). Then the output displacement X_V of the main spool is obtained according to Formulas (5) and (6). ΔP and X_V are input to the actuator together, then the output pressure P_b of

the actuator is obtained according to Formulas (8), (9) and (13). And finally the system simulation model is formed.

For the pressure servo valve, there are two common working conditions: step response and slope response. In this paper, the step response and slope response of brake pressure are used to evaluate the dynamic characteristics of the pressure servo valve. Given the 20 mA step current signal and 40 mA step current signal, the output response curves are shown in Figure 8a,b. Given the 40 mA ramp current signal shown in Figure 8c, the output response curve is obtained as shown in Figure 8d.

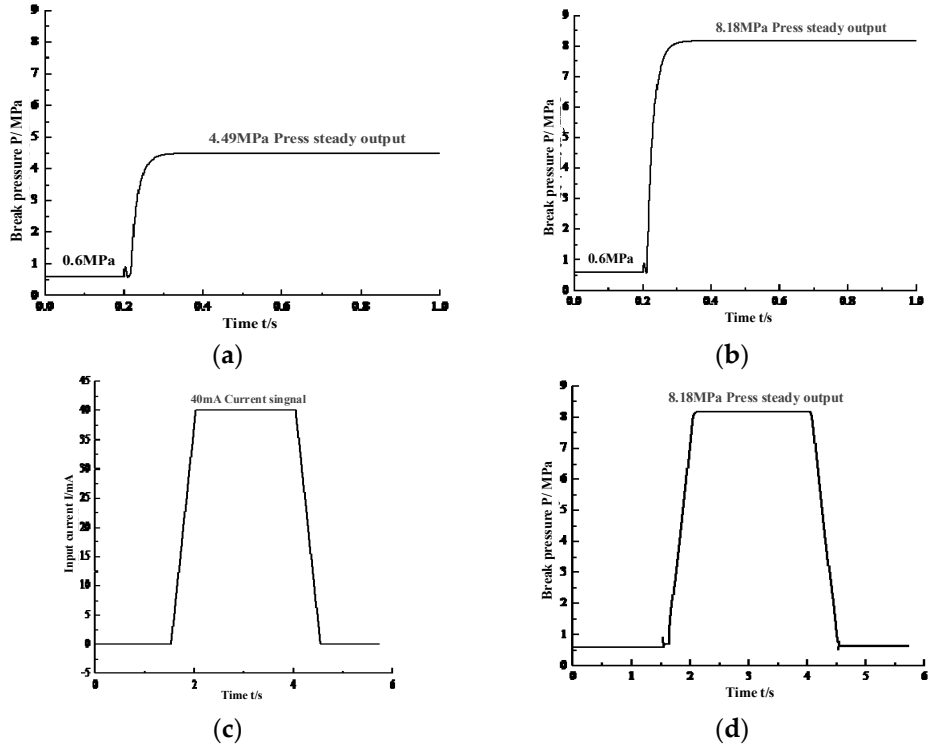

Figure 8. Simulation analysis of new brake pressure servo valve-actuator system. (**a**) 20 mA step brake pressure response. (**b**) 40 mA step brake pressure response. (**c**) 40 mA ramp input signal. (**d**) 40 mA ramp brake pressure response.

It can be seen that under the action of different input current, the TSBPSV testing system can quickly form stable output of brake pressure, and there is no obvious overshoot of brake pressure under various working conditions. Under the action of slope current, there is no oscillation phenomenon in the ascending and descending stages of brake pressure.

5. Experimental Verification of TSBPSV

5.1. Test Platform for Load Simulation Performance of Brake Pressure Servo Valve-Controlled Cylinder System

In order to verify the accuracy of the dynamic model of the two-stage brake pressure servo valve test system and the effectiveness of the brake pressure servo valve to suppress the vibration of the system. First of all, we developed the experimental scheme as shown in Table 2. Then, according to the principle of hydraulic system in Figure 2, an experimental platform for load simulation performance test of two-stage brake pressure servo valve test system and cylinder control system is built.

Table 2. Experimental scheme table.

Experimental Scheme	Signal Type	Change Time	Amplitude	Number
1	Step signal	0.2s	40mA	6
2	Slope signal	1.5s	40mA	6

The hardware in the loop simulation platform dSPACE is used in the experimental test, and the controller is developed by Universität Paderborn in Germany. The principle of valve-controlled system is shown in Figure 9. Through the interface of ControlDesk, the information exchange between dSPACE and PC can be realized. After the control algorithm is built in Matlab/Simulink, the target C code that can be recognized by the controller is generated automatically by using the code. Compared with the manual C code, the combination of MATLAB/Simulink and encoder can quickly design and test the control algorithm, avoid the complexity of the underlying C code, and improve the speed of the controller implementation stage.

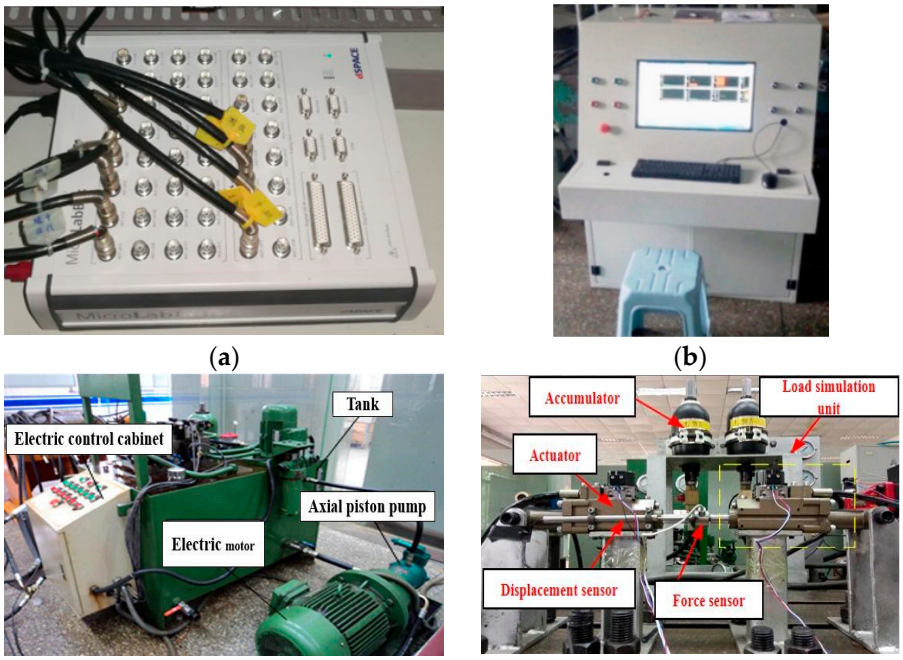

Figure 9. Test Platform for Load Simulation Performance of Braking Pressure Servo Valve-Controlled Cylinder System. (**a**) dSPACE controller. (**b**) Electric control cabinet. (**c**) Experimental station. (**d**) Experimental system organization.

The experimental platform used in this paper is a servo valve performance test platform. The controller, electric control cabinet of the experimental platform, the pumping station and performance test system of the experimental platform are shown in Figure 9.

The 25PCY14-1B quantitative axial piston pump is used in this experimental platform. If the oil supply pressure is set too high, the calorific value of the system will increase sharply. Therefore, from the perspective of experimental safety, the oil supply pressure of the experimental platform is set to 15 MPa. The basic parameters and objects of the experimental platform, such as hydraulic pipeline and load, are shown in Table 3 and Figure 9, respectively.

Table 3. Basic parameters of the experimental platform.

Oil Supply Pressure	System Flow	Brake Pipe	Return Pipe	Back Pressure	Load Stiffness	Load Damping
15 MPa	6.25×10^{-4} m^3/s	φ0.006 × 1.50 m	φ0.006 × 1.01 m	0.6 MPa	1,000,000 N/m	50 N·s/m

5.2. Test Experiment of TSBPSV

Under 20 mA step, 40 mA step and 40 mA slope current signals, the output pressure of the pressure servo valve is measured through experiments as shown in Figure 10.

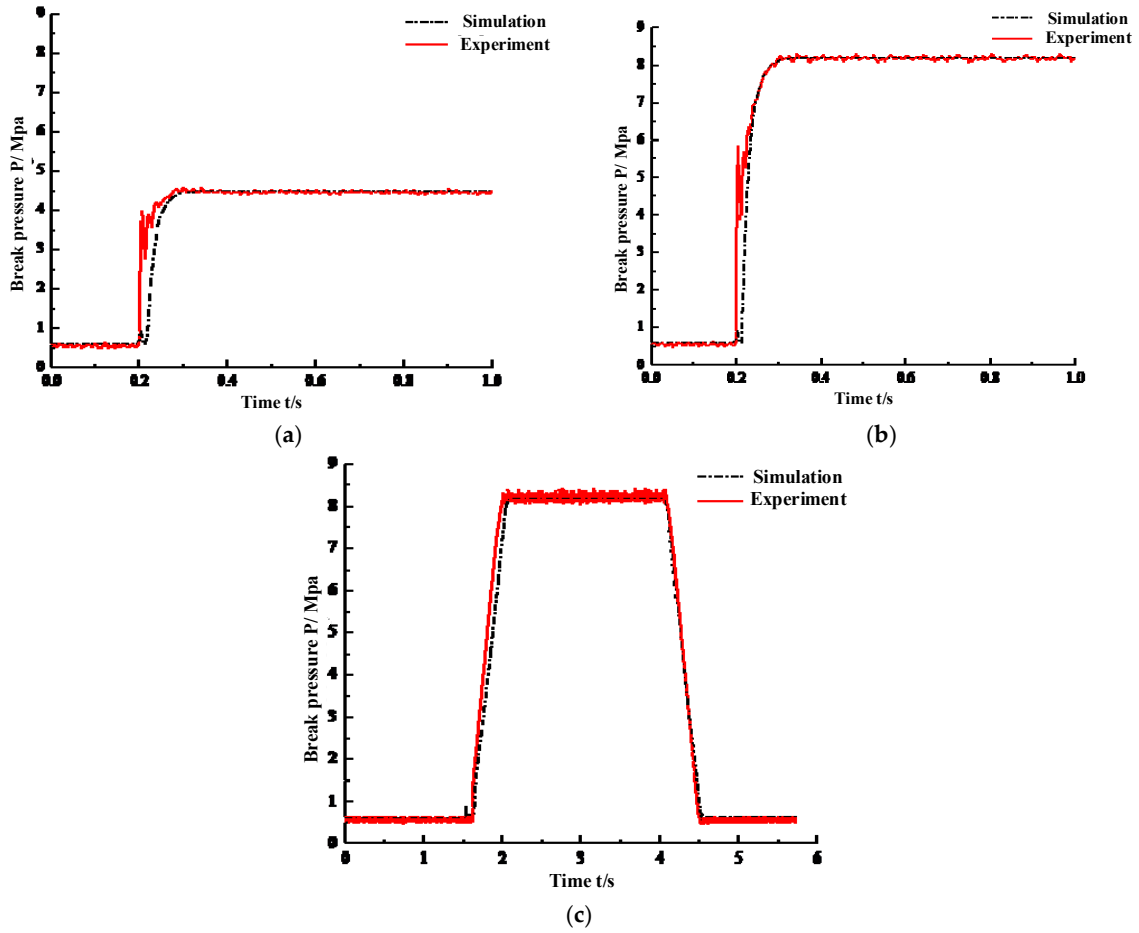

Figure 10. Experimental test results of TSBPSV. (**a**) 20 mA step current input. (**b**) 40 mA step current input. (**c**) 40 mA ramp current input.

It can be seen that the simulation results of the pressure servo valve are in good agreement with the experimental results in terms of brake pressure stability, rise time, overshoot and steady-state error. The establishment process of the load pressure of the jet nozzle in the simulation analysis is different from that in practice because of the comprehensive characteristic equation of the jet nozzle that is used in the simulation analysis model. This is the reason for the step of the simulation curve when t = 1.5. This leads to a certain error between the simulation results and the experimental results in the rising section of brake pressure.

The above experimental results show that the dynamic model of the TSBPSV test system has good analysis accuracy, and the brake pressure servo valve can provide a stable pressure output under various working conditions and the system does not show any obvious vibration phenomena.

5.3. Comparative Experiment of the TSBPSV and Prototypical Brake Pressure Servo Valve

In order to verify the effect of the TSBPSV, we compared with the prototypical brake servo valve. The results are shown in Figure 11. In order to verify the validity of the model, the response curves of two pressure servo valves are obtained under the condition of step signal. We analyzed the experimental contrast curve from two aspects.

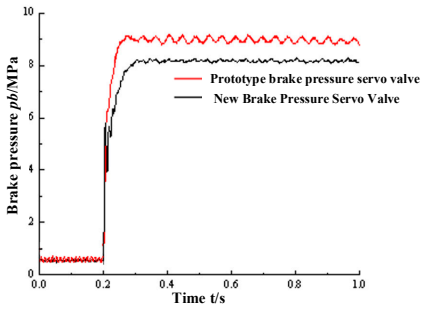

Figure 11. Comparison test curve of brake pressure between new servo valve and prototypical brake servo valve.

On the one hand, the difference of two curves is due to the structural difference of the two brake pressure servo valves. In the process of mathematical modeling, the mathematical expressions of brake pressure P_b are different.

Equation (5) is the dynamic equation of the power stage spool of the new brake pressure servo valve, and Equation (17) is the dynamic equation of the power stage spool of the prototype brake pressure servo valve, shown as follows:

$$(p_{b2} - p_h)A_c - K_{fg}(r\psi + x_c) - 2K_c x_c = M_c \frac{d^2 x_c}{dt^2} + B_c \frac{dx_c}{dt} \tag{17}$$

According to Equations (5) and (17), we get two more obvious expressions of output pressure written as Equations (18) and (19), as follows:

$$p_b = [p_L A_1 - M_v \frac{d^2 x_v}{dt^2} - B_v \frac{dx_v}{dt} - K(x_v + x_{v0}) - K_f x_v] \frac{1}{A_2} + p_h \tag{18}$$

$$p_{b2} = [M_c \frac{d^2 x_c}{dt^2} + B_c \frac{dx_c}{dt} + K_{fg}(r\psi + x_c) + 2K_c x_c] \frac{1}{A_c} + p_h \tag{19}$$

As can be seen from the above two equations, M_v and M_c, B_v and B_c, K_f and K_{fg} are different. This is the main reason why the stable values of the two curves P_b and P_{b2} are different.

On the other hand, the steady error of the prototype brake pressure servo valve is caused by the positive feedback of oil return in the structure. The steady error of the new brake pressure servo valve is caused by system noise. The formula of overshoot is $\sigma_p = \frac{C(t_p) - C(\infty)}{C(\infty)} \times 100\%$. The data in the Figure 11 can be used for calculation. The overshoot of the TSBPSV is 5%, and the overshoot of the prototypical valve is 20%. Therefore, the TSBPSV can suppress vibration compared with the prototype brake pressure servo valve.

6. Conclusions

Aiming at addressing the problem of output pressure jitter of common brake pressure servo valves, the TSBPSV is designed. The valve is provided with a feedback channel for the main valve spool. Theoretically, the negative feedback effect of the feedback channel on the spool movement makes the pressure output stable.

Firstly, a high-precision mathematical model of TSBPSV and test system is established. A dynamic simulation model is built. The step response and slope response were tested.

By comparing with the experimental curve of the prototypical servo valve, it is verified that the TSBPSV has a good vibration suppression effect.

Secondly, in order to verify the actual effect, the experimental platform of TSBPSV test system is built and verified. It shows that the mathematical model of the two-stage brake pressure servo valve. The test system established in this paper has high accuracy and can represent the actual physical system. And the designed two-stage pressure servo valve can suppress vibration.

At last, the mathematical model established in this paper can more accurately simulate the actual working situation. The paper also can provide a theoretical reference for the design of aircraft braking systems to suppress vibration.

Author Contributions: Conceptualization, L.Z. and Z.H.; methodology, C.F.; software, Y.W.; validation, Y.X., C.F. and Z.H.; formal analysis, X.K.; investigation, C.F.; resources, Z.H.; data curation, Y.W.; writing—original draft preparation, Y.X.; writing—review and editing, Z.H.; visualization, C.F.; supervision, X.K.; project administration, L.Z.; funding acquisition, L.Z. All authors have read and agreed to the published version of the manuscript.

Funding: This research was funded by Mathematical modeling and simulation analysis of aircraft lift system 6040186.

Conflicts of Interest: The authors declare no conflict of interest.

References

1. Vajargah, K.F. Evaluating the parametric, semi-parametric and nonparametric models for reliability in aircraft braking system. *Math. Sci.* **2020**, *12*, 20–32.
2. Zhang, X.; Liu, W.; Zhang, Y.; Zhao, Y. Experimental Investigation and Optimization Design of Multi-Support Pipeline System. *Chin. J. Mech. Eng.* **2021**, *34*, 33–53. [CrossRef]
3. Zhang, Y.; Jiang, W.; Zhu, Y.; Li, Z. Research on the Vertical Vibration Characteristics of Hydraulic Screw Down System of Rolling Mill under Nonlinear Friction. *Processes* **2019**, *7*, 792. [CrossRef]
4. Shang, X.; Zhou, H.; Yang, H. Improving Performance of a Resonant String-Based Pulsation Attenuator in Hydraulic Systems. *Appl. Sci.* **2020**, *10*, 8526. [CrossRef]
5. Kang, J.; Yuan, Z.; Tariq Sadiq, M. Numerical Simulation and Experimental Research on Flow Force and Pressure Stability in a Nozzle-Flapper Servo Valve. *Processes* **2020**, *8*, 1404. [CrossRef]
6. Lu, L.; Long, S.; Zhu, K. A Numerical Research on Vortex Street Flow Oscillation in the Double Flapper Nozzle Servo Valve. *Processes* **2019**, *7*, 721. [CrossRef]
7. Nam, S.; Lee, W.; Yoo, S.; Kim, K.; Chung, W.K. Development of Backdrivable Servovalve With Feedback Spring for Enhanced Electro-Hydraulic Torque Actuator. *IEEE Robot. Autom. Lett.* **2020**, *5*, 3145–3152. [CrossRef]
8. Chen, M.; Aung, N.Z.; Li, S.; Zou, C. Effect of Oil Viscosity on Self-Excited Noise Production Inside the Pilot Stage of a Two-Stage Electrohydraulic Servovalve. *J. Fluids Eng.* **2019**, *141*, 011106. [CrossRef]
9. Ni, T.W.; Yang, Z.-G. Failure analysis on unexpected leakage of electro-hydraulic servo valve in digital electric hydraulic control system of 300 MW thermal power plant. *Eng. Fail. Anal.* **2021**, *119*, 104992. [CrossRef]
10. Bi, H.X.; Yao, J.Y.; Li, Y. Research to the Wear and Geometric Error Relations of Electro hydraulic Servo Valve. *CEIS* **2011**, *15*, 1016. [CrossRef]
11. Zhang, Y.; Yuan, Z.; Wang, W. Force-fight problem in control of aileron'splane. *Comput. Modeling New Technol.* **2014**, *4*, 255–261.
12. Zhang, Y.; Yuan, Z. Control Strategy of Aileron's Force-fight. *Int. J. Multimed. Ubiquitous Eng.* **2018**, *8*, 301–312. [CrossRef]
13. Li, J.; Wang, Y.; Wang, X. Study of Electro-Hydraulic Force Servo System Based on Flow Press Servo-Valve and Fussy Intelligent Control Strategy. *J. Comput. Theor. Nanosci.* **2020**, *30*, e12419. [CrossRef]
14. Istanto, I.; Lee, I.; Huh, J. Controller Design for a Nozzle-flapper Type Servo Valve with Electric Position Sensor. *J. Drive Control.* **2021**, *16*, 29–35. [CrossRef]
15. Liu, C.; Wang, Y.; Pan, T.; Zheng, G. Fault diagnosis of electro-hydraulic servo valve using extreme learning machine. *Int. Trans. Electr. Energy Syst.* **2020**, *30*, e12419. [CrossRef]
16. Lyu, L.; Chen, Z.; Yao, B. Development of parallel-connected pump–valve-coordinated control unit with improved performance and efficiency. *Mechatronics* **2020**, *70*, 102419. [CrossRef]
17. Liu, G.; He, Z.; Bai, G.; Zheng, J.; Zhou, J.; Dai, B. Modeling and Experimental Study of Oil-Cooled Stacked Giant Magnetostrictive Actuator for Servo Valve. *Actuators* **2020**, *9*, 37. [CrossRef]
18. Saha, B.; Peng, J.; Li, S. Numerical and Experimental Investigations of Cavitation Phenomena Inside the Pilot Stage of the Deflector Jet Servo-Valve. *IEEE Access* **2020**, *8*, 64238–64249. [CrossRef]
19. Yang, H.; Wang, W.; Lu, K. Cavitation and flow forces in the flapper-nozzle stage of a hydraulic servo-valve manipulated by continuous minijets. *Adv. Mech. Eng.* **2019**, *11*, 1687814019851436. [CrossRef]

20. Zhao, J.; Zhou, S.; Lu, X. Numerical simulation and experimental study of heat-fluid-solid coupling of double flapper-nozzle servo valve. *Chin. J. Mech. Eng.* **2015**, *28*, 1030–1038. [CrossRef]
21. Zhang, Z.; Du, H.; Chen, S.; Huang, H. Frequency domain modeling, analysis and verification of electro-hydraulic servo steering system for heavy vehicles. *Proc. Inst. Mech. Eng. Part D J. Automob. Eng.* **2020**, *234*, 2836–2850. [CrossRef]
22. Liu, Y.; Wang, T.; Gong, G.; Gao, R. Present Status and Prospect of High-Frequency Electro-hydraulic Vibration Control Technology. *Chin. J. Mech. Eng.* **2019**, *32*, 1–16. [CrossRef]
23. Berri, P.C.; Dalla Vedova, M.D.L. A review of simplified servovalve models for digital twins of electrohydraulic actuators. *J. Phys. Conf. Ser.* **2020**, *1603*, 012016. [CrossRef]
24. Yan, H.; Jiang, B.; Zuo, Z. A hydraulic system based on the servo valve with dual input of machine and electricity. *Int. J. Model. Identif. Control* **2020**, *34*, 187–196. [CrossRef]
25. Wu, L.; Zhang, L.; Chen, K.; Zhan, C. Effect of key structures and parameters on dynamic characteristics of three-stage jet-pipe servo valve. *Iop Conf. Ser. Mater. Sci. Eng.* **2019**, *493*, 012161. [CrossRef]
26. Chu, Y.; Yuan, Z.; He, X.; Dong, Z. Model Construction and Performance Degradation Characteristics of a Deflector Jet Pressure Servo Valve under the Condition of Oil Contamination. *Int. J. Aerosp. Eng.* **2021**, *2021*, 8840084.